FBG SENSORS FOR PROCESS AND STRUCTURAL HEALTH MONITORING OF A SMALL TYPE III COMPOSITE OVERWRAPPED PRESSURE VESSEL FOR UNMANNED AERIAL VEHICLE

Helena, Rocha[a,b], Paulo, Antunes[b], Ugo, Lafont[c], João P., Nunes[a]

a: Institute for Polymers and Composites, University of Minho, Guimarães, Portugal
b: PIEP – Innovation in Polymer Engineering, Guimarães, Portugal – paulo.antunes@piep.pt
c: European Space Agency, Noordwijk, The Netherlands

Abstract: *In this work, fibre Bragg grating (FBG) sensors were embedded in a 1-litre type III composite overwrapped pressure vessel (COPV) for an unmanned aerial vehicle (UAV), during its manufacturing for process and structural health monitoring (SHM). A single optical fibre having eight FBG sensors was fixed around an aluminium liner to form a grid network. The carbon fibre/epoxy composite layers were wound on top of it with a winding machine. The FBG sensors were able to follow the developed strain during winding, making it an important quality control tool. The same sensors were used to monitor impact tests, where the distances between real and predicted locations varied between 17 and 56 mm.*

Keywords: *Composite Overwrapped Pressure Vessel;* Filament Winding; *Fibre Bragg Grating Sensor; Impact Damage; Structural Health Monitoring*

1. Introduction

Alternatives to fossil fuels are being explored, especially, for the transportation sector, aiming to restrain global warming [1]. Hydrogen-powered fuel cell systems are regarded as one viable energy alternative solution [2]. Particularly, when compared to electrical batteries, Unmanned Aerial Vehicles (UAV) may benefit from it for longer flight times and autonomy, with short charging time, keeping downtime to a minimum [1]. The implementation of fuel cell systems usually utilizes Composite Overwrapped Pressure Vessels (COPV) for hydrogen storage. COPV are the most weight efficient solution among pressure vessels, where a fibre reinforced polymer composite overwrap is wound around a liner [3].

COPV may face some reliability issues due to the loading scheme complexity, the assortment of commercial construction solutions and material degradation. Yet, traditional non-destructive testing may fail to timely detect critical defects that may occur in between periodic inspections. Differently, COPV instrumentation and application of Structural Health Monitoring (SHM) systems offers added safety, as continuous data acquisition enables the real-time detection of critical defects. Hence, immediate repair, operation status downgrade or deactivation of the COPV can be instructed to prevent catastrophic bursting. Additionally, COPVs are also susceptible to low velocity impacts (LVI), causing barely visible impact damage (BVID). BVID can result in stiffness deterioration, which may reduce the lifetime of the COPV [4].

A small type III COPV was designed resorting to FEA and experimental burst testing was used for validation. The integration of FBG sensors in the COPV was demonstrated for winding process monitoring and further impact testing monitoring of the produced COPV.

 ©2022 Antunes et al. doi:10.5075/epfl-298799_978-2-9701614-0-0 published under CC BY-NC 4.0 license

2. Experimental Techniques

2.1 Design and Production of Smart COPV

A small COPV consisting of a 6061-T6 aluminium liner and a carbon fibre/epoxy composite overwrap was developed to withstand a nominal storage pressure of 350 bar. The COPV has a 1 litre volume capacity and internal diameter of approximately 75 mm. The layup configuration of the composite overwrap was optimized via FEA, using Abaqus 2020 software, with the burst testing being simulated. The COPV was modelled to have a burst pressure that is 3 times that of the nominal storage pressure (1050 bar). CADWIND software was used to find adequate winding patterns for the mentioned liner, which were used in the FEA model. This was an iterative process between the layup configuration (winding angles and number of layers) and the resultant modelled burst pressure. The Hashin failure criteria was used to identify damage initiation in the composite overwrap. The optimized configuration was found to be $[90_3/\pm15_2/90_3]$. Burst pressure tests were performed on three COPVs, according to the EN12245 European standard, to validate the FEA model. The obtained burst pressure was 1061 ± 26 bar.

An optical fibre with a FBG sensor array was fixed in the aluminium liner with X120 epoxy adhesive from HBM and left to cure at room temperature. Each optic fibre had 8 FBG sensors, with central wavelengths ranging from approximately 1535 to 1564 nm, each separated by about 4 nm. The optic fibres were polyimide coated with a diameter of 150 µm and having FC/APC connectors. The optic fibres were supplied by HBK FiberSensing, Portugal. The optic fibre was wound around the central cylindrical region of the liner. The OF at the FBG position was fixed at 90° to be aligned with the carbon fibres in the first circumferential layer, while the OF in between FBG sensor was wound at lower angles to decrease the length of the OF. The FBG sensors were distanced in a way that they were positioned in 3 lines along the longitudinal axis of the liner, equally separated by an angle of 120°, where each following sensor was placed in the next line, separated by 26 mm in the longitudinal direction of the liner from the previously fixed sensor, forming an equally distributed network grid (see figure 1).

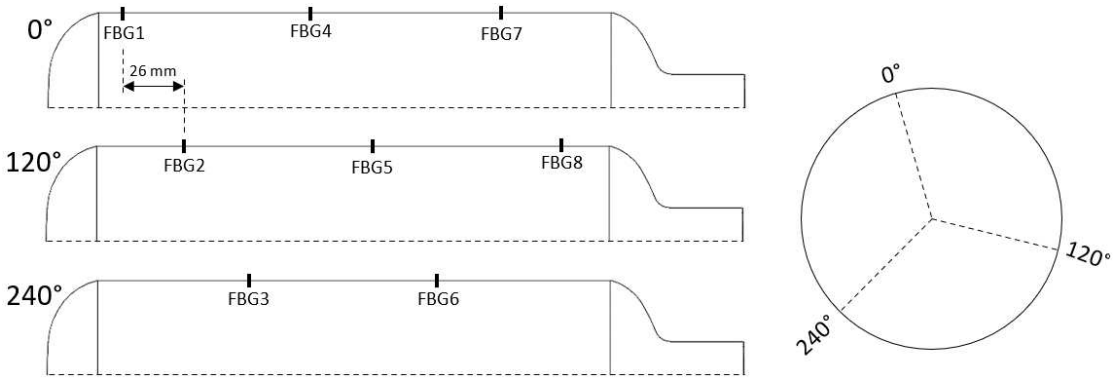

Figure 1: Schematic representation of FBG sensors on the liner surface

Winding process monitoring can be a valuable tool for quality control. The winding pre-tension plays an important role on the stiffness of the composite overwrap; lower winding pre-tension may not allow to use the full potential of tensile strength of the carbon fibres, while excessive pre-tension may cause fibre damage. A 150 mm long screw was adhesively bonded to the closed dome of the liner to attach the optic fibre interrogator and monitor the winding process (see figure 2(a)). The interrogator system, from Ibsen Photonics, comprised the DL-BP1 1501A super-

 ©2022 Antunes et al. doi:10.5075/epfl-298799_978-2-9701614-0-0 published under CC BY-NC 4.0 license

luminescent LED source and I-MON 256 USB High Speed interrogation monitor. The system has a wavelength fit resolution of 0.5 pm and acquired the FBG data during winding at a sampling rate of 50 Hz.

A filament winding machine, manufactured by Gislotica, Portugal, was used to produce the COPV. The filament winding machine has six axes of movement: three linear moving axes and two rotating axes of the carriage, and a rotating spindle, where the liner is fixed. Part program files were also generated by CADWIND software for each pattern (circumferential, helical and angle combinations) and fed to the winding machine. The prepreg tape was wound over the optic fibre on the liner surface to produce the composite overwrap. A 6 mm wide prepreg tape made of Tenax®-E ITS50 carbon fibre, from Teijin, and RCX0125 epoxy, from RED Composites, was used. After winding, the COPVs were cured with an initial holding stage at 90 °C for 60 min and a last holding stage at 150 °C for 90 min, as per suggestion of the resin manufacturer. An example of a produced COPV, with embedded FBG sensors, is shown in figure 2(b).

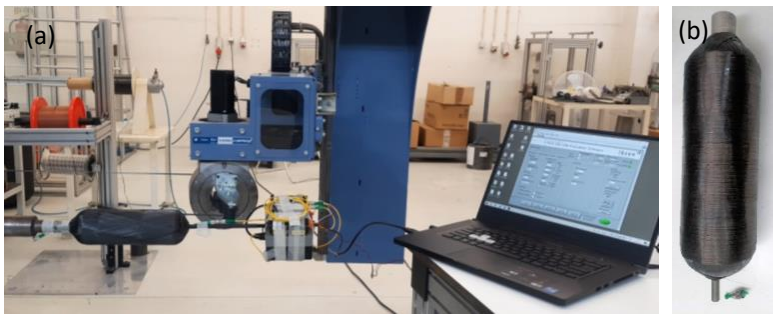

Figure 2: Production of the COPV by tape winding

2.4 Impact Testing and Localization

Drop-weight impact tests were performed on the Fractovis Plus impact testing equipment from CEAST. The impactor had a hemispheric shape with a 20 mm diameter and a mass of 5.045 Kg. Each COPV was impacted at 4 locations. The low velocity impacts were performed with the impactor head at an initial vertical distance of 305 mm and velocity of 2.446 m/s, to produce an impact energy of 15 J. The optical fibre data acquisition during impacts was taken at a sampling rate between 550 and 800 Hz, depending on the exposure time used in the interrogation system. The setup used for impact testing can be seen in figure 3.

Figure 3: Drop-weight impact testing setup with optical interrogation system

 ©2022 Antunes et al. doi:10.5075/epfl-298799_978-2-9701614-0-0 published under CC BY-NC 4.0 license

A simple residual strain amplitude method, similar to the one reported by Hiche et al. [5], was used to predict damage location on the circumferential section of the COPV. This method is based on the assumption that FBG sensors closer to the impact sight measure higher residual strain.

The residual strain values on each sensor, after impact, were normalized to calculate the strain ratio, r_{ij}, between each pair of sensors, according to Eq. 1.

$$r_{ij} = \frac{\bar{\varepsilon}_j}{\bar{\varepsilon}_j + \bar{\varepsilon}_i} \quad (1)$$

being $\bar{\varepsilon}_j$ and $\bar{\varepsilon}_i$ the normalized absolute maximum strain obtained from FBG_i and FBG_j sensors, respectively.

For the detection of each impact, only the four sensor pairs with highest strain magnitude, M_{ij}, were used (Eq. 2).

$$M_{ij} = \bar{\varepsilon}_j + \bar{\varepsilon}_i \quad (2)$$

The FBG sensors coordinates (ρ, ϕ, z) were initially inputted using cylindrical coordinate system. The linear surface distance between each of the selected sensor pairs, d_{ij}, was calculated following Eq. 3.

$$d_{ij} = \sqrt{\left(z_j - z_i\right)^2 + \left(\left(\Phi_j - \Phi_i\right)\left(\frac{\pi\rho}{180}\right)\right)^2} \quad (3)$$

The relative distance between FBG_i of the FBG_i/FBG_j sensors pair and the expected impact location, I_d, was calculated according to Eq. 4.

$$I_d = r_{ij} \times d_{ij} \quad (4)$$

The cartesian coordinates of the relative impact locations ($(I_{ij})_x$, $(I_{ij})_y$) were recorded, using the nearest FBG sensor as origin of the coordinate axes, considering the 2D flat projection of the cylinder region (as in figure 1(b)). The cartesian coordinates of the predicted impact location, ($I(p)_x$, $I(p)_y$), is finally obtained from the average of the relative impact positions of the four FBG sensor pairs previously selected, as given by Eq. (5).

$$\left[I(p)_x, I(p)_y\right] = \left[\frac{\sum_{k=1}^{4}\left(I_{ij}^k\right)_x}{4}, \frac{\sum_{k=1}^{4}\left(I_{ij}^k\right)_y}{4}\right] \quad (5)$$

3. Results and Discussion

3.1 Winding Process Monitoring

Figure 6 shows the strain variation measured by FBG4 during winding process. Up to approximately 10 minutes there are three main strain decreasing steps corresponding to the three wound internal circumferential layers. When the carbon fibres cover the FBG sensor, there is a sudden decrease of strain, followed by a strain plateau during the remaining time of layer winding, until the FBG is compressed again in the next wounded layer. The winding of the helical layers does not impose further compression on the FBG sensor (time between approximately 10 and 50 min), and instead there is a slight increase of strain during these steps. Next, three

 ©2022 Antunes et al. doi:10.5075/epfl-298799_978-2-9701614-0-0 published under CC BY-NC 4.0 license

sudden strain decreasing steps are also observable during winding of the external layers. At the moment that the carbon fibre covers the FBG the steep decrease of strain occurs, but it quickly recovers to a strain value similar to the one after winding of the helical layers, approximately -90 με. By the end of the winding process the FBG shows a strain of approximately -100 με. All the FBG sensors showed a very similar behaviour.

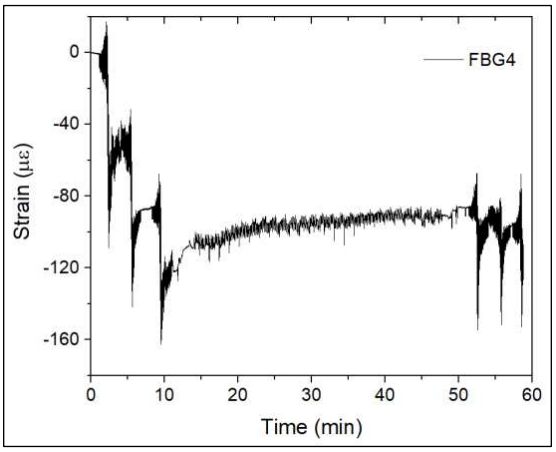

Figure 6: Strain change measured by FBG4 during COPV winding process

3.2 Impact Detection and Localization

The strain amplitude method explained in section 2.4 was used to locate impact events, based in the residual strain after impact. Figure 7 shows the location of the FBG sensors, “real” impact locations, predicted impact locations based on the residual strain between pairs of FBG sensors and averagely predicted impact location. Distances as small as 17 mm and up to 56 mm (Table 1) were measured between the predicted impact locations and the “real” impact locations. This proved to be a simple and inexpensive method to closely find the impact location. It should be mentioned that differences between the “real” and the predicted impact location may arise due to the misidentification of the FBG sensors location in the COPV after winding. The FBGs are fixed in the liner surface and a plastic jig mask is used to mark their position. However, after winding, as the diameter of the COPV increased comparatively to the liner diameter, an exact identification of the FBG sensors is not possible. After production of the COPV, only one of the three longitudinal lines with three sensors is marked on the surface of the COPV using the plastic jig mask, while the remaining sensor locations are identified by reference measurements on the COPV surface considering the 120° angle between each longitudinal line and the 26 mm longitudinal distance between consecutive sensors.

 ©2022 Antunes et al. doi:10.5075/epfl-298799_978-2-9701614-0-0 published under CC BY-NC 4.0 license

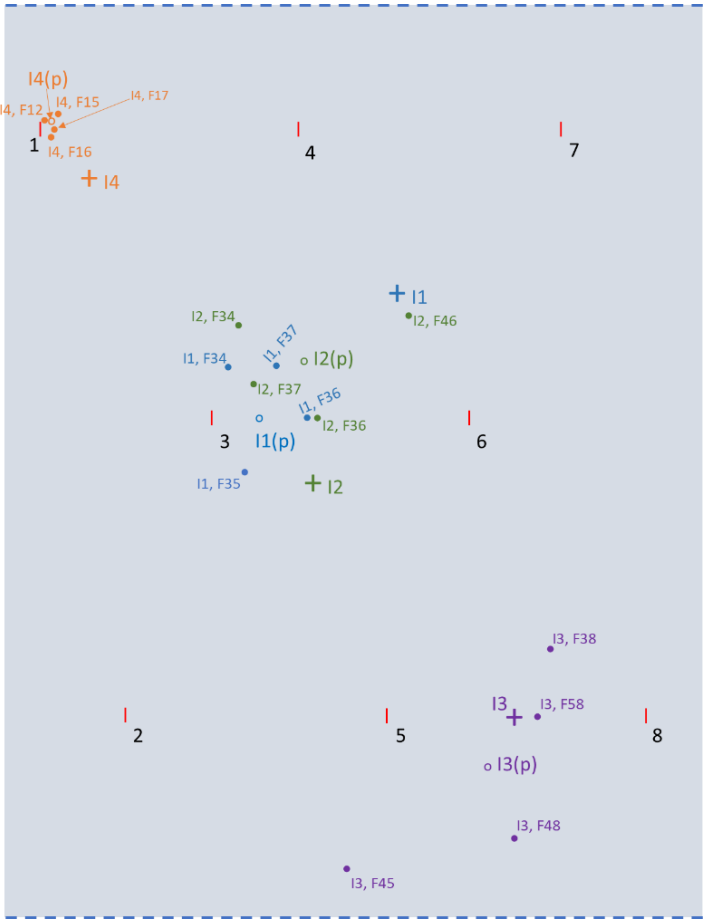

Impact	Real – Predicted distance (mm)
1	56
2	36
3	17
4	21

+ In - Impact location of impact number n

o In(p) - Average Impact location prediction

• In, F_{ij} - Impact location prediction between FBG sensors pair F_{ij}

Figure 7: Real and predicted Impact locations on the flat projection of the COPV cylindric region

4 Conclusions

An FBG sensor grid, consisting of 8 FBG sensors, was integrated in a small type III COPV for winding process monitoring and LVI detection and localization. The optical fibre with FBG sensors was wound around the cylindrical region of the liner to distribute the FBG sensors over this surface area. The FBG data clearly allows to identify the winding step of each layer. The winding of the inner circumferential layers produced a compression strain of about 130 με, while the strain slightly increases during winding of the helical layers. Further compressive strains are visible when winding the outer circumferential layers, where a final compressive strain of approximately 100 με is measured. The integration of the FBG sensors array in the liner is a valuable strategy to monitor the full production process, serving as a quality control tool.

After production completion of the COPV, the same FBG sensors were used to monitor LVI. A strain-amplitude based method was used to locate impact damage in between FBG sensor pairs. The used method was able to localize damage, with distances between the “real” impact location and the predicted impact location varying between 17 and 56 mm. These are short distances that would quickly enable the localization of the impact in a real life structure and to take preventive measures.

 ©2022 Antunes et al. doi:10.5075/epfl-298799_978-2-9701614-0-0 published under CC BY-NC 4.0 license

Acknowledgements

Helena Rocha would like to acknowledge the support of European Space Agency [Network/Partnering Initiative Program - ESA Contract 4000123315] and the ACE project founded by the European Union's Portugal 2020 founding program.

5 References

1. Pollet BG, Kocha SS, Staffell I. Current status of automotive fuel cells for sustainable transport. Curr Opin Electrochem. 2019;16:90–5.
2. Menon NC, Kruizenga AM, Alvine KJ, Marchi CS, Nissen A, Brooks K. Behaviour of Polymers in High Pressure Environments as Applicable to the Hydrogen Infrastructure. In: Proceedings of the ASME 2016 Pressure Vessels and Piping Conference. Vancouver; 2016. p. 1–14.
3. Abdalla AM, Hossain S, Nisfindy OB, Azad AT, Dawood M, Azad AK. Hydrogen production, storage, transportation and key challenges with applications: A review. Energy Convers Manag. 2018;165(April):602–27.
4. Weerts RAJ, Cousigné O, Kunze K, Geers MGD, Remmers JJC. A methodological approach to model composite overwrapped pressure vessels under impact conditions. Compos Struct [Internet]. 2021;276(December 2020):114482. Available from: https://doi.org/10.1016/j.compstruct.2021.114482
5. Hiche C, Coelho CK, Chattopadhyay A. A strain amplitude-based algorithm for impact localization on composite laminates. J Intell Mater Syst Struct. 2011;22(17):2061–7.

 ©2022 Antunes et al. doi:10.5075/epfl-298799_978-2-9701614-0-0 published under CC BY-NC 4.0 license